

Data-driven Vector-measurement-sensor Selection based on Greedy Algorithm

Yuji Saito^{1*}, Taku Nonomura^{1*}, Koki Nankai^{1*}, Keigo Yamada^{1*} and Keisuke Asai^{1*}

¹Department of Aerospace and Engineering, Tohoku University, Miyagi 980-8579, Japan

Yasuo Sasaki^{2*}, and Daisuke Tsubakino^{2**}

²Department of Aerospace and Engineering, Nagoya University, Nagoya, Aichi, 464-8603, Japan

*Non-Member, IEEE

**Member, IEEE

Manuscript received , 2019; revised , 2020; accepted , 2020. Date of publication , 2020; date of current version , 2020.

Abstract—A vector-measurement-sensor problem for the least square estimation is considered, by extending the previous novel approach in this paper. Previous studies show that the sparse-sensor-placement algorithm in which the state of the flowfield can be obtained by the limited number of sensors for the flowfield that can be represented by the limited POD mode. The extension of the vector-measurement-sensor selection of the greedy algorithm is proposed and is applied to test and PIV (particle image velocimetry) data to reconstruct the full state based on the information given by the sparse vector-measurement sensors.

Index Terms—Data processing, sensor placement, greedy algorithm, vector-measurement.

I. INTRODUCTION

Reduced-order modeling for fluid analysis and flow control gathers a lot of attentions. With regard to reduced-order modeling, proper orthogonal decomposition (POD)[1], [2] is one of the effective methods to decompose the high-dimension fluid data into several significant modes of flow fields. Here, POD is a data-driven method which gives us the most significant and relevant structure in the data, and it exactly corresponds to principal component analysis and Karhunen-Loeve (KL) decomposition, where the decomposed modes are spatially orthogonal each other. The POD analysis for discrete data matrix can be carried out by applying the singular value decomposition, as is often the case in the engineering fields. Although there are several advanced data-driven methods, dynamic mode decomposition[3], [4], empirical mode decomposition, and others which include efforts by the authors[5], [6], this research is only based on POD which is the most basic data-driven method for reduced-order modeling.

If the data, such as flow fields, can be effectively expressed by limited numbers of POD modes, the limited sensors placed at appropriate positions gives us the approximated full state information. This effective observation might be one of the keys for flow control and flow prediction. This idea has been adopted by Manohar et al.[7], and the sparse-sensor-placement algorithm has been developed and discussed. The idea here is expressed by the following equation:

$$\begin{aligned} \mathbf{y} &= \mathbf{H}\mathbf{U}\mathbf{x} \\ &= \mathbf{C}\mathbf{x} \end{aligned} \quad (1)$$

Here, $\mathbf{y} \in \mathbb{R}^p$, $\mathbf{x} \in \mathbb{R}^r$, $\mathbf{H} \in \mathbb{R}^{p \times n}$ and $\mathbf{U} \in \mathbb{R}^{n \times r}$ are the observation vector, the POD mode amplitude vector, the sparse sensor location matrix, and spatial POD modes, respectively. In addition, p , n , and r are the number of sensors, the degree of freedom of the spatial POD modes, and the rank for truncated POD, respectively. The problem above is considered to be one of the sensor selection problems when \mathbf{U} is assumed to be a sensor-candidate matrix. Thus far, this sensor selection

problem has been solved by the convex approximation and the greedy algorithm, where the greedy algorithm was shown to be much faster than the convex approximation algorithms. Table 1 summarizes the computational costs based on each calculation methods: brute-force searching, convex approximation method, greedy algorithm, respectively. Previous study [7] introduced that the greedy algorithm is based on QR-discrete-empirical-interpolation method [8], [9] when the number of sensors is the same as that of POD mode and its extension for the least square problem when the number of sensors is greater than that of POD modes. Both convex approximation and greedy algorithm work pretty well for the sensor selection problems. However, in the greedy algorithm, the theoretical background for calculation is not clear when the number of the sensor is greater than that of POD modes. Therefore, the problem, the number of sensors is greater than that of POD modes, will not be a subject in this study.

TABLE 1. Computational cost of sensor selection methods[7].

	Computational cost
Brute-force search	$\frac{n!}{(n-p)!p!} \sim O(n^p)$
Convex approximation method	$O(n^3)$ per iteration.
Greedy method	$p \leq r : O(nr^2)$ $p > r : O(n^3)$

There are several applications of a vector-measurement sensor, such as two components of velocity of particle image velocimetry, or simultaneous velocity, pressure and temperature measurements used in weather forecasting. For instance, we have now been developing a sparse processing PIV-measurement system [10]. The real-time PIV measurement of the flow field should be required to perform active control of the high speed flow field in the laboratory experiments. The velocity field is calculated from the cross-correlation coefficient for each interrogation window of the particle image in PIV-measurement, but the amount of windows that can be processed in a short time is limited. The number of processing data is reduced and the flow field is estimated by a limited the number of selected windows located sparsely as in this study. This method can achieve the real-time measurement of the high speed flow.

The extension of the vector-measurement-sensor selection of the convex approximation has already been addressed in the original

Corresponding author: Yuji Saito (e-mail: saito@aero.mech.tohoku.ac.jp).

Associate Editor: Alan Smithe.

Digital Object Identifier 10.1109/LENS.2017.0000000

paper[11], while one of the greedy algorithms has not been conducted. The sensor selection of very high dimension with such a constraint should be resolved in reasonable time scale when the real-time measurement and flow-control or flow prediction would be conducted. Therefore, the extension of the greedy sparse sensor selection method with the vector-measurement sensors is straightforwardly proposed and it is applied to test and PIV data to reconstruct the full state based on the information given by the sparse vector-measurement sensors. It should be noted that the robustness against changes in POD modes should be considered because the POD mode is not always constant in the actual flow field. However, this point is out of scope of this study and left for future study. We focus to propose the greedy algorithm for the vector-measurement-sensor problem of the constant POD modes as the first step of the series of studies in this study, whereas the assumption of the constant POD modes is the same as that in the previous study.[7]

II. MATERIAL AND METHODS

A. PIV Measurement

The PIV measurement for acquiring time-resolved data of flow fields around an airfoil was conducted previously.[12] Here, the experimental data are briefly explained. The wind tunnel testing was conducted in Tohoku-university Basic Aerodynamic Research Wind Tunnel (T-BART) with a closed test section of 300 mm × 300 mm cross-section. The airfoil of the test model has an NACA0015 profile, the chord length and span width of which are 100 mm and 300 mm, respectively. The freestream velocity U_∞ and attack angle of the airfoil α were set to be 10 m/s and 16 degree, respectively. The chord Reynolds number was 6.4×10^4 . The time-resolved PIV measurement was conducted with the double-pulse laser. The time between pulses, the sampling rate, the particle image resolution and the total number of image pairs were 100 μ s, 5000 Hz, 1024 × 1024 pixels, and $N = 1000$, respectively. The tracer particles were 50% aqueous solution of glycerin with estimated diameter of a few micrometers. The particle images were acquired by using the double pulse laser (LDY-300PIV, Litron) and a high-speed camera (SA-X2, Photron) which were synchronized each other.

B. Previous Greedy Algorithm for Scalar-Measurement Sensors

In the greedy algorithm based on QR decomposition for scalar measurement problem, i -th sensor is chosen where

$$i = \arg \max \|v_i\|_2^2. \quad (2)$$

Here, $v_i = [V_{i,1} V_{i,2} \dots V_{i,r}]$, and $V_{ij} = V$ is initialized to be U for $p = r$ sensor conditions, respectively. Given i index, the V matrix is pivoted and QR decomposition is conducted. After that, the next sensor is chosen for remaining matrix. The algorithm for $p = r$ sensors is QR-discrete-empirical-interpolation method (QDEIM)[9].

The optimization is considered to conduct the maximization of the determinant of the C matrix to stably solve x vector. The select of the sensor position is based on maximizing the norm of the corresponding row vector of the sensor-candidate matrix. Although the round-off error increases, this procedure can be written by Gram-Schmidt orthogonalization with choosing the rows of the largest norm. Algorithm 1 shows the algorithm implemented in this study for

the replacement of QR decomposition by Gram-Schmidt procedure. Although the calculation algorithm for the condition $p > r$ has already been proposed in the previous study (which corresponds to the use of $V = UU^T$ instead of $V = U$)[7], the vector extension of this algorithm was not conducted in this study because the validity of the algorithm has not been explained and clarified well in the previous study. This point is left for the future research.

Algorithm 1 Greedy method for the scalar-measurement sensors

```

procedure GREEDY METHOD FOR THE SCALAR-MEASUREMENT SENSORS
  ( $a, b$ )
    Set sensor-candidate matrix  $V = U$ .
     $p = r$ 
    for  $k = 1, \dots, p$  do
       $v_i = [V_{i,1} V_{i,2} \dots V_{i,r}]$ 
       $i \leftarrow \arg \max \|v_i\|_2^2$ 
       $V \leftarrow V - V v_i^T v_i / \|v_i\|_2^2$ 
       $H_{k,i} = 1$ 
    end for
    return  $H$ 
end procedure

```

C. Proposed Greedy Method for Vector Measurement Sensors Algorithm

In the vector measurement, we consider the following equation:

$$y = \begin{bmatrix} H & 0 & 0 & 0 \\ 0 & H & 0 & 0 \\ 0 & 0 & \ddots & 0 \\ 0 & 0 & 0 & H \end{bmatrix} \begin{bmatrix} U_1 \\ U_2 \\ \vdots \\ U_s \end{bmatrix} x \quad (3)$$

$$= \begin{matrix} & H_s & U & x \end{matrix} \quad (4)$$

$$= \begin{matrix} & C & x \end{matrix} \quad (4)$$

Here, $U_k \in \mathbb{R}^{\frac{n}{s} \times r}$ is a k th vector component of a sensor candidate matrix, $H \in \mathbb{R}^{p \times \frac{n}{s}}$ is the sensor location matrix for each vector component. Here, s is the number of components of the measurement vector. Again, p , n , and r are the number of sensors, the degree of freedom of the spatial POD modes including the different vector components, and the rank for truncated POD modes, respectively. This arrangement of data is intentionally chosen with considering the situation when the data matrix of $X = [X_u^T \ X_v^T]^T$ is applied and the spatial POD modes of X is used as the sensor-candidate matrix, where X_u^T and X_v^T are data matrices of x -velocity component and y -velocity component in PIV data, respectively. This arrangement does not matter for the Gram-Schmidt procedure, but we recommend to reorder the data as the data of the same vector-measurement sensor are gathered in successive rows when this algorithm is further straightforwardly extended by block-pivoting and block-QR algorithm for eliminating round-off error. However, the latter extension is not addressed in this short note, for brevity.

Fig. 1 shows that the vector-measurement sensor placement problem can be seen as the restriction on the choice of sensor of H_s matrix in the sense of (3). Similar to the scalar-measurement, the next sensor can be chosen to maximize the determinant of C matrix. Because the multiple (s) rows of U matrix are chosen simultaneously by selecting one point in the vector version, the hypervolume of

selected row vectors is maximized, instead of the norm of the row vector in the scalar version. This hypervolume (square root of J_i in the algorithm) can be simply computed by the Gram-Schmidt-like procedure by multiplying the norm of one row and removing its component from other selected rows in order. After choosing the sensors, the components of selected row vectors are subtracted from the sensor-candidate matrix and then proceed to the next sensor placement selection. The algorithm is summarized in Algorithm 2. The extension of the convex approximation method[11] for the vector sensor placement are addressed in the original paper, and it is adopted in present test case.

Algorithm 2 Greedy method for Vector-measurement sensors

procedure GREEDY METHOD FOR VECTOR-MEASUREMENT SENSORS
ALGORITHM(a, b)

Set sensor-candidate matrix U_j for j th vector component measurement.

$$U = [U_1^T \ U_2^T \ \dots \ U_r^T]^T$$

$$sp = r$$

$$V = U$$

for $k = 1, \dots, p$ **do**

for $i = 1, \dots, n$ **do**

$$v_i = [V_{i,1} \ V_{i,2} \ \dots \ V_{i,r}]$$

end for

for $i = 1, \dots, \frac{n}{s}$ **do**

$$J_i = 1$$

$$\tilde{V} = V$$

for $j = 1, \dots, s$ **do**

$$J_i = J_i \|(\tilde{v}_{i+\frac{n}{s}(j-1)}\|_2^2$$

$$\tilde{V} \leftarrow \tilde{V} - \tilde{V}(\tilde{v}_{i+\frac{n}{s}(j-1)}^T \tilde{v}_{i+\frac{n}{s}(j-1)} / \|\tilde{v}_{i+\frac{n}{s}(j-1)}\|_2^2)$$

end for

end for

$$i = \arg \max J_i$$

$$H_{k,i} = 1$$

for $j = 1, \dots, s$ **do**

$$v_{i+\frac{n}{s}(j-1)} = [V_{i+\frac{n}{s}(j-1),1} \ V_{i+\frac{n}{s}(j-1),2} \ \dots \ V_{i+\frac{n}{s}(j-1),r}]$$

$$V \leftarrow V - V(v_{i+\frac{n}{s}(j-1)}^T v_{i+\frac{n}{s}(j-1)} / \|v_{i+\frac{n}{s}(j-1)}\|_2^2)$$

end for

end for

return H

end procedure

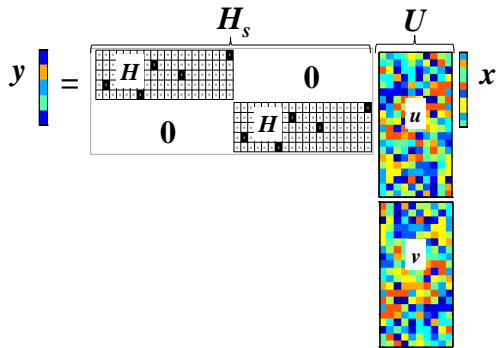


Fig. 1. Graphical image on (3) in vector-measurement sensor problem ($s = 2$)

III. RESULTS AND DISCUSSIONS

A. Random sensor problem

Numerical experiments are conducted and the proposed algorithm is validated for the vector-measurement sensor placement problem in the multiple components of the measurement vector ($s = 2$). The random sensor candidate matrices, $U_1 \in \mathbb{R}^{1000 \times r}$ and $U_2 \in \mathbb{R}^{1000 \times r}$ were set, where each component of the matrices is given by Gaussian distribution of $\mathcal{N}(0, 1)$. Therefore, the sensor candidate matrix U is expressed as $U = [U_1^T U_2^T]^T$ in this validation. The sparse sensor location matrix are calculated based on each method; random selection, convex approximation method, and greedy algorithms of vector-measurement and scalar-measurement sensors, respectively. The greedy algorithm of scalar-measurement sensors selects $r/2$ sensors based on one sensor candidate matrix as opposed to the greedy algorithm of vector-measurement sensors which selects $r/2$ sensors based on both sensor candidate matrices. After selecting sensors, the logarithm of the determinant of $C = HU$ is calculated using both sensor candidate matrices. Therefore, the other components of the vector-measurement sensors are randomly selected because they are not considered in the process of sensor selections. Of course, the greedy algorithm of scalar-measurement is not considered to succeed to select sensors due to a lack of proper treatment in the other components of a vector-measurement sensor candidate matrix. Fig. 2 shows the relationship between the number of sensors and the logarithm of the determinant of $C = HU$. Here, greedy (vector), greedy (U_1 -scalar), and greedy (U_2 -scalar) in Fig. 2 are calculation results based on the greedy algorithm for vector-measurement sensors using U_1 and U_2 , that for scalar-measurement sensors using U_1 , and that for scalar-measurement sensors using U_2 , respectively. All plots are average values of 100 calculations changing U_1 and U_2 as a normal random number every calculation. Fig. 2 shows that the values of C obtained by vector greedy algorithm are highest value in all calculation results in all sensor and POD mode conditions. Because both greedy (U_1 -scalar) and greedy (U_2 -scalar) calculate sensor placements using only U_1 or U_2 although the sensor candidate matrix U consists of U_1 and U_2 , the half of sensor components of the greedy method for the scalar-measurement sensors has almost the same quality as the sensor placement obtained by the random selection. Therefore, all the results of the logarithm of the determinant of the greedy method for scalar-measurement sensors are in between those of the greedy method for vector-measurement sensors and of the random selection. The optimization is considered to conduct the maximization of the determinant of the C matrix to stably solve x vector as explained in II.B. Therefore, the greedy (vector) algorithm is more effective for sparse sensor placement than the greedy (scalar) and convex relaxation in multiple components of the measurement ($s = 2$).

B. PIV measurement

The reduced-order PIV data are reconstructed by sparse sensors that are chosen by several methods. Here, the PIV data for flows around airfoils are adopted, and the truncated POD modes r are preconditioned. The extended convex approximation method is called a convex (vector) method, for brevity. The greedy algorithm for scalar-measurement and vector-measurement sensors of u and v field is applied. These methods are called a greedy (vector), a greedy (u -scalar), and a greedy (v -scalar) methods for brevity.

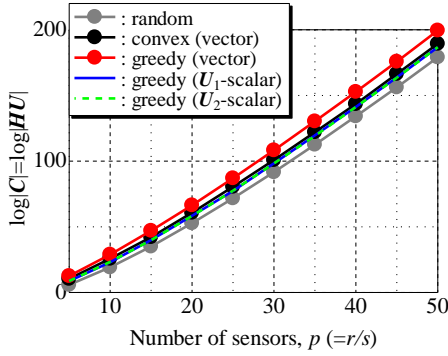


Fig. 2. Relationship between the number of sensor and the logarithm of the determinant of C ($s = 2$)

Fig. 3 shows the relationship between the reconstruction error e and the number of sensors p , obtained by full observation (a black solid line with close circle), random selection (a gray solid line with close circle), convex (vector) (a blue solid line with close circle), greedy (vector) (a red solid line with close circle), greedy (u -scalar) (a red dot line), and greedy (v -scalar) methods (a red solid line). The reconstruction is based on the linear least squares method and it is written with the C matrix as follows:

$$\mathbf{x}_i^{\text{reconst}} = \mathbf{C}^{-1} \mathbf{y}_i \quad (5)$$

Here, the reconstruction error e is introduced for quantitative evaluation of flow field reconstruction.

$$e = \sqrt{\frac{\sum_{i=1}^r \sum_{j=1}^N (x_{i,j} - x_{i,j}^{\text{reconst}})^2}{\sum_{i=1}^r \sum_{j=1}^N x_{i,j}^2}}. \quad (6)$$

The reconstruction error of full observation and greedy (vector) decreases as the number of sensors increases. On the other hand, the reconstruction error of the random selection, the convex (vector) approximation method and both greedy (u -scalar and v -scalar) algorithms do not decrease as the number of sensors increases. The greedy (u -scalar and v -scalar) algorithms determine the sensors in only one field in u or v field. Therefore, the half of the reconstructed field obtained by greedy (u -scalar and v -scalar) algorithms is the same to the reconstructed field obtained by the random selection and the reconstruction error of the greedy (scalar) algorithm follows that of the random selection. Because the convex approximation method always does not select optimal sensors, the reconstruction error of the convex (vector) approximation does not decrease with increases the number of sensors and POD modes as Fig. 2 also shows.

IV. CONCLUSIONS

The greedy method extended to vector-measurement sensor problems, such as the sensor placement problem in PIV data of fluid dynamic fields, is introduced and investigated in this paper. The sensor selection problem is solved by the convex approximation method for vector sensor and greedy methods for both scalar-measurement and vector-measurement sensors, where greedy algorithms are shown to be much faster than the convex approximation algorithms. The proposed method was validated using the random sensor problem before adopted to PIV data, and the calculation result shows that the proposed method is more effective for the sparse vector-measurement sensor placement than the greedy method for scalar-measurement sensors and the

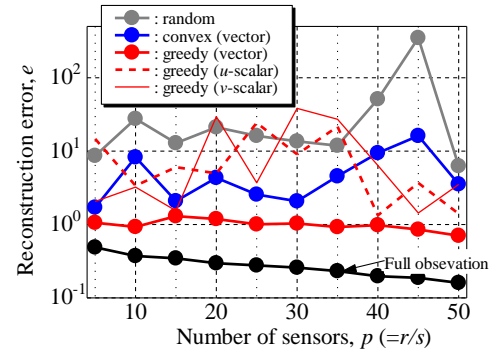


Fig. 3. The relationship between the number of sensors and the reconstruction error

convex approximation method for the vector-measurement sensors. The calculation results of PIV data show that the reconstruction error of the greedy method for the vector-measurement sensors is smaller than other methods in ($r = ps$). Therefore, the greedy method extended to the vector-measurement sensor problem is illustrated to be more effective sparse sensing than other methods.

ACKNOWLEDGEMENTS

T.N. is supported by the grant JPMJPR1678 of JST Presto.

REFERENCES

- [1] G. Berkooz, P. Holmes, and L. J. Lumley, "The proper orthogonal decomposition in the analysis of turbulent flows," *Annual Review of Fluid Mechanics*, vol. 25, no. 1971, pp. 539–575, 1993.
- [2] K. Taira, S. L. Brunton, S. T. Dawson, C. W. Rowley, T. Colonius, B. J. McKeon, O. T. Schmidt, S. Gordeyev, V. Theofilis, and L. S. Ukeiley, "Modal analysis of fluid flows: An overview," *AIAA Journal*, pp. 4013–4041, 2017.
- [3] P. J. Schmid, "Dynamic mode decomposition of numerical and experimental data," *Journal of Fluid Mechanics*, vol. 656, no. July 2010, pp. 5–28, 2010.
- [4] J. N. Kutz, S. L. Brunton, B. W. Brunton, and J. L. Proctor, *Dynamic mode decomposition: data-driven modeling of complex systems*. SIAM, 2016, vol. 149.
- [5] T. Nonomura, H. Shibata, and R. Takaki, "Dynamic mode decomposition using a kalman filter for parameter estimation," *AIP Advances*, vol. 8, p. 105106, 2018.
- [6] —, "Extended-kalman-filter-based dynamic mode decomposition for simultaneous system identification and denoising," *PloS one*, vol. 14, p. e0209836, 2019.
- [7] K. Manohar, B. W. Brunton, J. N. Kutz, and S. L. Brunton, "Data-driven sparse sensor placement for reconstruction: Demonstrating the benefits of exploiting known patterns," *IEEE Control Systems Magazine*, vol. 38, no. 3, pp. 63–86, June 2018.
- [8] S. Chaturantabut and D. C. Sorensen, "Nonlinear model reduction via discrete empirical interpolation," *SIAM Journal on Scientific Computing*, vol. 32, no. 5, pp. 2737–2764, 2010.
- [9] Z. Drmac and S. Gugercin, "A new selection operator for the discrete empirical interpolation method—improved a priori error bound and extensions," *SIAM Journal on Scientific Computing*, vol. 38, no. 2, pp. A631–A648, 2016.
- [10] N. Kanda, K. Nankai, Y. Saito, T. Nonomura, and K. Asai, "Feasibility study on sparse processing particle image velocimetry," *Bulletin of the American Physical Society*, 2019.
- [11] S. Joshi and S. Boyd, "Sensor selection via convex optimization," *IEEE Transactions on Signal Processing*, vol. 57, no. 2, pp. 451–462, 2009.
- [12] K. Nankai, Y. Ozawa, T. Nonomura, and K. Asai, "Linear reduced-order model based on piv data of flow field around airfoil," *TRANSACTIONS OF THE JAPAN SOCIETY FOR AERONAUTICAL AND SPACE SCIENCES*, vol. 62, no. 4, pp. 227–235, 2019.